MAŁGORZATA SKORUPA*, TOMASZ MACHNIEWICZ*, ADAM KORBEL*,
ANDRZEJ SKORUPA*

RIVET FLEXIBILITY AND LOAD TRANSMISSION FOR A RIVETED LAP JOINT

Presented in this paper are results of an experimental investigation on the rivet flexibility and load transmission in a riveted lap joint representative for the aircraft fuselage. The test specimens consisted of two aluminium alloy Alclad sheets joined with 3 rows of rivets. Two different squeeze forces were applied to install the rivets. Rivet flexibility measurements have been performed under constant amplitude fatigue loading using several methods including two original optical techniques developed by the present authors. The axial tractions in the sheets required to determine the rivet flexibility have been derived from strain gauge measurements. In order to eliminate the effect of secondary bending the strain gauges have been bonded at the same locations on the outside and faying surface of the sheet. The experiments enabled an evaluation of the usefulness of various techniques to determine the rivet flexibility. It was observed that, although the measured flexibility was identical for both end rivet rows, the load transfer through either of these rows was different. Previous experimental results by the present authors suggest that behind the non-symmetrical load transfer distribution through the joint are large differences between the rivet hole expansion in the sheet adjacent to the driven rivet head and the sheet under the manufactured head [1]. It has been concluded that commonly used computation procedures according to which the load transfer is only related to the rivet flexibility may lead to erroneous results.

1. Introduction

The knowledge of stresses within a riveted joint is a fundamental step in estimating its fatigue life and damage tolerance characteristics. In order to approach the problem of stress conditions at the rivet holes the distribution of loads acting in the joint must be known. The role of a rivet is to transfer the load from one sheet to another in the overlap region. For a configuration with

---

* *AGH University of Science and Technology, Al. Mickiewicza 30, 30-059 Kraków, Poland; E-mail: machniew@agh.edu.pl*

more than one row of the rivets the applied force P is split at the first row into the bypass load (T_{BP}), which remains in the sheet, and the transfer load (T_{TR}) transmitted to the other sheet, as schematically shown in Fig. 1. The T_{TR}-load is comprised of the bearing force (T_{BR}) resulting from the bearing pressure exerted by the rivet shank on the hole surface and the friction force (T_{FR}) induced by friction between the mating sheets. Friction is localized mainly beneath the rivet heads where the maximum clamping occurs.
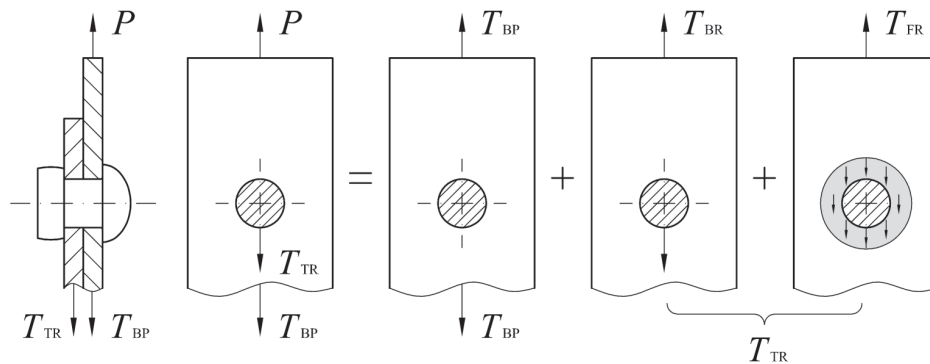

Fig. 1. Axial forces in sheets of a two-layer lap joint

As shown in Fig. 2 for an overlap of two sheets with r rivet rows, the internal axial forces in the sheets can be computed by considering the displacement compatibility between the sheets and rivets, Eq. (a), and the equilibrium condition for each transverse section of the overlap, Eq. (b). The elongations of the sheets (Δ) and the rivet deflections between the sheets (δ) can be expressed in terms of the tractions in the sheets (T) through Eqs (c) and (d). In Eq. (c) $(EA)_j$ is the longitudinal rigidity of sheet j, whilst f_i in Eq. (d) is the flexibility of rivets in row "i". The early interest in fastener flexibility measurements has been caused by the intention to calculate the load transfer distribution in joints with multiple fastener rows using the above procedure.

$$l_i + \Delta_{1,i} + \delta_{i+1} = l_i + \Delta_{2,i} + \delta_i \tag{a}$$

$$T_{1,i} + T_{2,i} = P \text{ with } T_{1,0} = T_{2,r} = P \text{ and } T_{2,0} = T_{1,r} = 0 \tag{b}$$

$$\Delta_{j,i} = T_{j,i} l_i / (EA)_j \tag{c}$$

$$\delta_i = (T_{1,i-1} - T_{1,i}) f_i \tag{d}$$
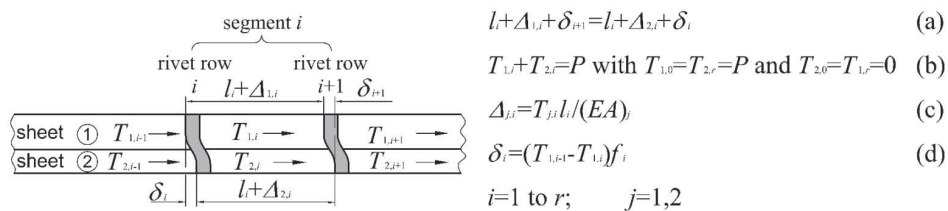
$$i = 1 \text{ to } r; \qquad j = 1,2$$

Fig. 2. Cut out from a multiple rivet row lap joint and equations for the computation of axial forces in the sheets

Presented in this paper are measurement results on the rivet flexibility and load transmission for a lap joint representative for the aircraft fuselage. Two values of the rivet squeeze force have been considered. Because literature data on the rivet flexibility show a very large spread, as evidenced by comparisons between empirical formulas on rivet flexibility produced in [2,3], several methods of rivet flexibility measurements have been applied and evaluated in the present investigation. The load tractions in the sheets observed in the experiments have been compared with those computed according to the equations given in Fig. 2.

2. Specimens

The rivet flexibility and load transfer were measured during constant amplitude fatigue loading (S_{min}=12 MPa, S_{max}=120 MPa) on simple riveted lap joint specimens assembled from two D16 Alclad 2 mm thick sheets using 5 mm dia. round head AD rivets. For each of a total of two specimens tested, the rivets were squeezed with a different force to obtain the D/D_o ratio of 1.3 and 1.5, where D and D_o is the diameter of the rivet driven head and rivet shank, respectively. The overlap configuration is shown in Fig. 3a.

Besides the riveted specimens a monolithic specimen of the same Al alloy and dimensions shown in Fig. 3b was also used in some methods of the rivet flexibility measurements, as detailed in the next section.
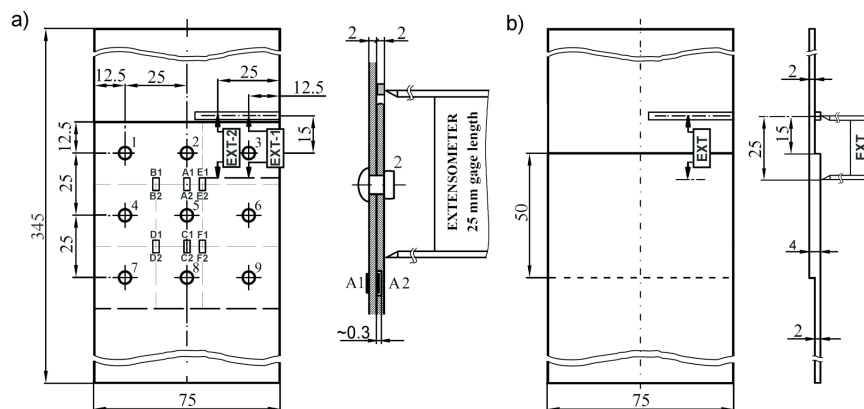

Fig. 3. Specimens for rivet flexibility and load transfer measurements: (a) riveted specimen; (b) dummy specimen

3. Rivet flexibility measurements

The rivet flexibility measurements should ensure that, as far as possible, the measured results be not influenced by the secondary bending of the sheets as this effect is not accounted for in the computation of the rivet flexibility from the measurement data (cf. Fig. 2). For long overlaps the specimen extension between the clamping edges and then the average rivet flexibility value for the joint can be derived from records of the machine displacement gauge (LVDT transducer), Fig. 4a, provided that the component resulting from the compliance of machine elements is subtracted from the measured displacement value (Δl). The middle rivet rows may show a different deflection response than the fatigue critical end rows because the middle rows undergo much more uniform bearing pressure than the end rows where the maximum moment due to secondary bending occurs. In order to measure the flexibility for the end rivet rows the extensometer can be positioned as shown in Fig. 3a. At that short gauge length, however, the sheet curvature due to secondary bending should be accounted for because the difference between the displacements measured at the outer surface and those occurring at the faying surface can be of the same order of magnitude as the rivet deflection. Figs 4b and c show the principle of optical measurements of the rivet flexibility, not affected by secondary bending, proposed by the present authors. The technique further referred to as the edge method, Fig. 4b, enables the determination of the rivet deflection in the end row from the measured relative displacement between the mating sheets at the overlap edge: $\Delta y = y_{max} - y_{min}$, where the distances y_{max} and y_{min} correspond to the maximum and minimum load of the fatigue cycle. Because Δy is in the order of 10^{-2} mm, a high accuracy measurement system is required. The method presented in Fig. 4c, further referred to as the reference element technique, is applicable to rivets in both the end and inner rows. The effect of secondary bending is compensated by using a reference element which is a piece of wire bonded to the sheet surface next to the rivet head. The difference between the displacements of the rivet head on either side of the overlapping sheets, Δy_1 and Δy_2, results not only from the deflection of the rivet (δ) but also from its rotation (φ) caused by the bending deformation of the sheets:

$$\Delta y_2 = \Delta y_1 + \varphi h + \delta. \tag{1}$$

In order to determine angle φ the displacement of the reference element tip (Δy_3) was additionally measured. The length of this element (h) was the same as the distance between the rivet heads which implies

$$\Delta y_3 = \Delta y_1 + 2\varphi h + \delta. \tag{2}$$

Based on Eqs (1) and (2) the rivet deflection was determined as

$$\delta = 2\Delta y_2 - \Delta y_1 - \Delta y_3; \qquad (3)$$

where the quantities Δy_i represent displacements between the minimum and maximum level of the loading cycle.

All above mentioned techniques have been applied in the present experiments. As shown in Fig. 3a, the extensometer was mounted at locations EXT-1 and EXT-2 in order to measure the end row rivet flexibility along the rivet column and midway between the columns. Both these locations were also considered when the optical edge method, Fig. 4b, was used.
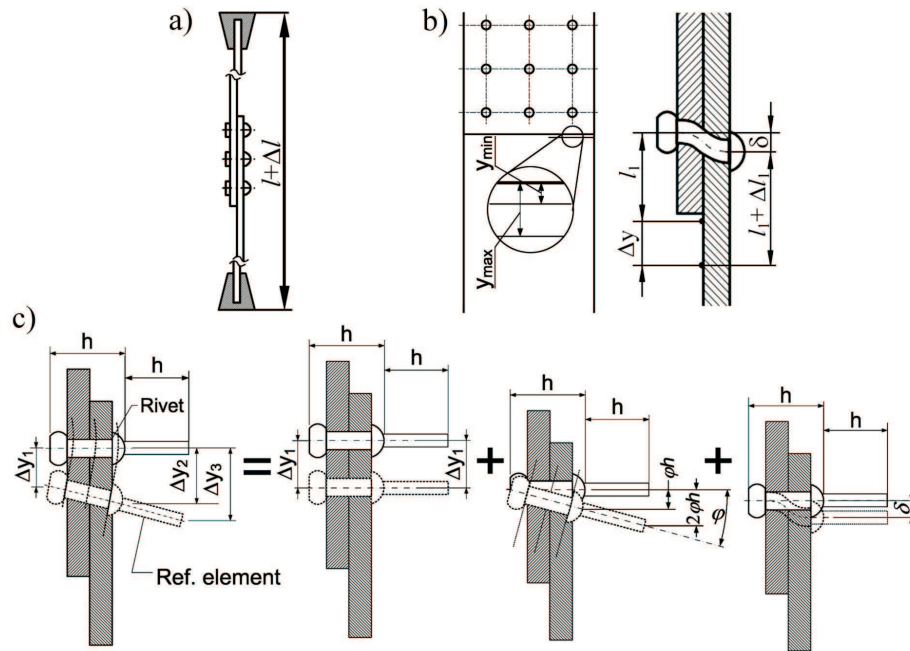

Fig. 4. Various techniques for rivet flexibility measurements: (a) LVDT transducer measurements; (b) edge method; (c) reference element method

As said above, with the reference element method the rivet deflection can be directly derived. When other techniques were used, two approaches were applied in an attempt to extract the rivet deflection from the measured data. One of these referred to as the analytical compensation involved subtracting from the measured extension appropriate sheet elongations computed from the Hook law (cf. Eq. (c), Fig. 2). In the case of the LVDT transducer records this analytical compensation can only eliminate the sheet extension between the specimen clamping edges but it is not capable of eliminating the deflection of the machine components included in the measurement data.

With the other approach, referred to as the experimental compensation and applicable only in the case of the extensometer measurements and the LVDT transducer records, the extensions measured for the monolithic dummy specimen shown in Fig. 3b were subtracted from those acquired for the riveted specimens. It was believed that this concept makes it possible to eliminate also the contribution of the machine compliance in the LVDT transducer records.

The axial tractions in the sheets needed to compute the sheet elongations and the rivet compliance using Eqs (c) and (d) respectively (cf. Fig. 2) were determined from strain gauge measurements, as detailed in the next section.

The results on both the rivet flexibility and load transfer were determined from averaged measurement data on strains, extensions or displacements recorded during three consecutive load cycles. The data acquisition was repeatedly performed throughout the fatigue test.

Comparisons between some results on the rivet flexibility derived for the D/D_o=1.3 specimen are presented in Fig. 5. For clarity, only the data captured along a single rivet column are shown in the case of the extensometer measurements and the edge method. Slightly higher f-values midway between the columns compared to those along the columns, were only detected using the edge method and solely for the D/D_o=1.3 specimen. The measurements indicated a good repeatability of results taken for various rivets in a given row and symmetry of the flexibility values for both end rows. It can be seen in Fig. 5 that the optical methods and the extensometer measurements coupled with the analytical compensation yield similar results for the rivets in the end rows. Altogether, the measurement data for both the D/D_o=1.3 and D/D_o=1.5 specimen have indicated that the scatter of the f-values measured using the considered three methods for the rivets in the end rows is within ±10%. Behind the differences between the results from these three techniques can be simplifications involved in computing the sheet extension, like neglecting the stress concentration and, in the case of the extensometer measurements, ignoring the sheet curvature due to the secondary bending. Note also that the accuracy of the optical measurement setup used in this investigation (±2 μm) equals several per cent of the measured deflection values. Especially in the case of the reference element method, which involves measurements of three small quantities, a somewhat higher resolution of the optical system would be desired. Only the reference element method makes it possible to measure f for the middle row. The data obtained from this technique reveal a lower flexibility of rivets in that row compared to the flexibility measured for the end rows, as also evidenced in Fig. 5 by the

results for rivets in the middle row consistently lower than for rivets in the end row.

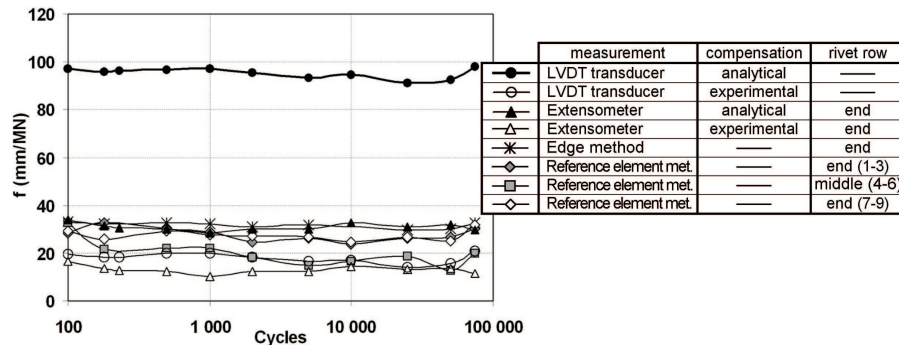| measurement	compensation	rivet row
LVDT transducer	analytical	——
LVDT transducer	experimental	——
Extensometer	analytical	end
Extensometer	experimental	end
Edge method	——	end
Reference element met.	——	end (1-3)
Reference element met.	——	middle (4-6)
Reference element met.	——	end (7-9)

Fig. 5. Exemplary results on rivet flexibility from several measurement techniques

The effect of the fatigue loading on the flexibility behaviour was found to depend on the squeeze force level. In the case of the D/D_o=1.3 specimen an insignificant decrease of the flexibility during the fatigue loading was observed only for rivets in the middle row. For the D/D_o=1.5 specimen a moderate decrease in f occurred also for the end rows. After 100 000 cycles the rivet flexibility became reduced by 20%. A decrease in the joint flexibility during both constant amplitude and variable amplitude fatigue loading has also been reported by Jarfall [3].

Whilst the extensometer measurements and both optical methods provide the flexibility for a specific rivet, the results derived from the LVDT transducer records represent the average rivet flexibility of the joint. Fig. 5 demonstrates that compared to other measurement techniques the latter method coupled with the analytical compensation which does not cover the deformation of the machine parts yields an over threefold overestimate of the rivet flexibility. Thus, the present results offer the explanation for the overestimation of the rivet flexibility by the Morris [2] formula based on the same measurement technique. On the other hand, the data in Fig. 5 imply that the experimental compensation leads to an underestimate of the flexibility values because the average results from the LVDT transducer records and, especially, the extensometer measurement results for the end rows are even below the flexibilities measured for the middle row. Evidently, the deformation of the dummy specimen cannot properly represent the deformation of the sheets in the riveted specimen.

In Table 1, the measured rivet flexibility values averaged over the initial 75 000 load cycles for either specimen and the corresponding load transfer ratios computed for the measured f-values according to the procedure from Fig. 2 are given. It is seen that due to the lower difference between the

flexibility for the end and middle rivet row in the case of the D/D_o=1.5 specimen the computed load transmission through the joint is for that specimen more levelled of than for the D/D_o=1.3 specimen. The computed T_{TR}/P ratio, higher for the middle row than for end rows, is reflective of the lower f-value for this row.

Table 1.

Measured rivet flexibilities and computed load transfer ratios for end and middle rivet rows

D/D_o	f_{end}(mm/MN)	f_{middle}(mm/MN)	$T_{TR,end}/P$	$T_{TR,mid}/P$
1.3	26.7	16.4	0.293	0.414
1.5	18.1	12.8	0.314	0.327

4. Measurements of tractions in the sheets

In order to measure the axial loads in the sheets the riveted specimens were instrumented with twelve strain gauges A1, A2 to F1, F2, Fig. 3a. For joints with eccentricities, like the lap joints, the measured axial stresses indicate a combined effect of the axial loads and secondary bending. The stresses contributed by the axial tractions were obtained as the average of the stresses measured by the gauges bonded at the same location at the outer and faying surface of the sheet adjacent to the manufactured rivet heads, as shown for gauges A1 and A2 in Fig. 3a. It is seen that bonding the gauges at the faying surface required that a 0.3 mm deep recess for each gauge had to be machined in the mating sheet. Also, about 0.3 mm deep slots were milled in that sheet to lead out the gauge wiring. In either of the two transverse sections considered in the measurements the gauge located midway between the rivet columns indicated nearly the same stress as the gauge located at a distance of 6.25 mm from the column, i.e. the stress measured at location B equalled that measured at location E and the stress at location D was the same as that at location F. Considering above, the axial tractions in the sheets have been computed by integrating the stress distributions schematized as shown in Fig. 6a, where the measured stresses are specified as a percentage of the tensile stress applied on the joint. It is seen in Fig. 6a that, compared to the D/D_o-ratio of 1.3, the stress distribution corresponding to D/D_o=1.5 is more levelled off as in the latter case the differences between the stress value at the rivet column and between the columns are lower in both sections. This observation is consistent with the results of Terada [4] measured using a thermo-elastic analyser.

Integrating the measured stress field presented in Fig. 6a yields the distribution of the load transfer ratio through the joint shown in Fig. 6b. Here,

a most striking feature is the non-symmetrical load transmission by the end rivet rows. For both the D/D_o=1.3 and D/D_o=1.5 specimen load T_{1-3} transferred from the sheet adjacent to the rivet manufactured head to the sheet adjacent to the driven head is lower than load T_{7-9} transmitted at the other end row, i.e. from the sheet next to the driven head to the sheet under the manufactured head. The difference in the load transfer distribution by the end rows is more pronounced for the D/D_o=1.3 than for the D/D_o=1.5 specimen for which the load transmission through all three rows is more homogeneous.
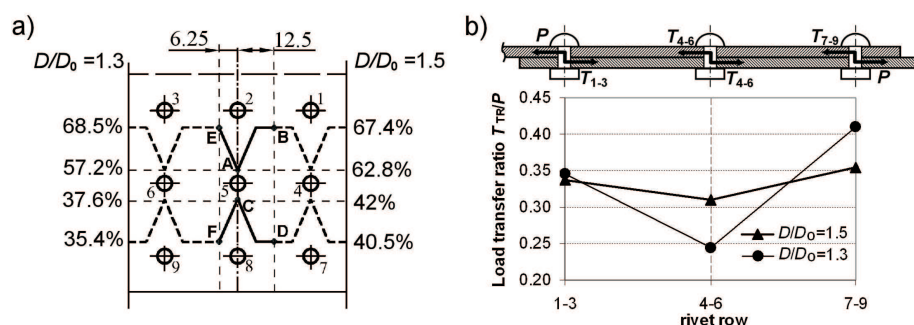

Fig. 6. Transfer load measurement results: (a) schematization of the stress distributions in the transverse sections between the rivet rows; (b) load transfer ratios for the lap joint

5. Discussion and conclusions

The non-symmetrical load transfer observed experimentally is not reflected by the rivet flexibility measurements which for either of the two specimens provide identical results on f for both end rivet rows. Presumably, the large differences between the hole expansion in the sheet adjacent to the driven head and in the sheet next to the manufactured head revealed in experimental [1,5] and numerical [6,7] studies are behind the non-symmetrical load transfer distribution by the end rivet rows. Note also in Fig. 6b that the measured load transfer distribution between the end and middle row exhibits a different trend than the computed results given in the last two columns in Table 1. Whilst due to the lower flexibility measured for the middle row the computed transfer ratio for that row is higher than for the end rows, the measured load transfer values show an opposite behaviour. It can be concluded that because the flexibility is not the only factor which affects the load transmitted by the rivet the computation procedure illustrated in Fig. 2 may not provide a quantitatively and even qualitatively correct solution on the internal forces in the sheets.

The measured results on the load transfer shown Fig. 6b can back up observations by the present authors on the fatigue failure location in fatigue

tests on lap joint specimens same as in this study except that six rivets in a row were installed. For all of a total of four specimens riveted with squeeze forces leading to the D/D_o-ratios ranging from 1.3 to 1.4 the fatigue crack nucleation and fracture occurred in the sheet adjacent to the rivet driven head, when the applied cyclic stresses were the same as in the present experiments. However, under the same applied stresses the D/D_o=1.5 specimens fractured in the sheet next to the manufactured head. Though the hole expansion is always larger in the sheet under the driven head than under the manufactured head [1,5], for the D/D_o=1.3 specimen the negative effect of the high transfer load in the sheet adjacent to the driven head evidently overwhelms the beneficial effect of the larger hole expansion in that sheet. For the D/D_o=1.5 specimen the load transfer is more homogeneous (cf. Fig. 6b). Moreover, due to the higher clamping pressure between the sheets resulting from a higher rivet squeeze force the friction force picks up more load than for D/Do=1.3. Consequently, for the D/D_o=1.5 specimen the bearing force values at the end rivet rows do not differ significantly and the effect of hole expansion dominates.

REFERENCES

[1] Skorupa M., Skorupa A., Machniewicz T., Korbel A.: An experimental investigation on the fatigue performance of riveted lap joints, Proc. of the 25th Symposium of the International Committee on Aeronautical Fatigue (ICAF 2009), 2009, pp. 449-473.

[2] Morris G.: Defining a standard formula and test-method for fastener flexibility in lap-joints, Ph.D. Thesis, TU Delft, The Netherlands, 2004.

[3] Jarfall L.: Shear loaded fastener installation. Int. J. Vehicle Design, 1986, 7, pp. 337-379.

[4] Terada H.: A proposal on damage tolerant testing for structural integrity of aging aircraft – learning from JAL accident in 1985. Fracture mechanics, 1985, 25, pp. 557-570.

[5] Skorupa M., Skorupa A., Machniewicz T., Korbel A.: Effect of production variables on the fatigue behaviour of riveted lap joints. International Journal of Fatigue, 2010, 32, pp. 996-1003.

[6] Rans C.D.: The role of rivet installation on the fatigue performance of riveted lap joints, Ph.D. Thesis, Carleton University, Ottawa 2007.

[7] Müller R.P.G.: An experimental and analytical investigation on the fatigue behaviour of fuselage riveted lap joints. The significance of the rivet squeeze force, and a comparison of 2024-T3 and Glare 3, Ph.D. Thesis, TU Delft, The Netherlands, 1995.

Podatność nitów oraz transfer obciążenia w nitowanych połączeniach zakładkowych

S t r e s z c z e n i e

W artykule zaprezentowano wyniki eksperymentalnych badań podatności nitów oraz transferu obciążenia w nitowanych połączeniach zakładkowych, typowych dla kadłuba samolotu. Badania prowadzono przy stałej amplitudzie obciążenia, na blachach z lotniczego stopu aluminium D16 połączonych trzema rzędami nitów przy dwóch różnych siłach ich zakuwania. Do pomiaru podatności nitów zastosowano kilka różnych metod w tym zaproponowane przez autorów dwie oryginalne metody optyczne. Porównanie uzyskanych dzięki nim wyników umożliwiło ocenę użyteczności poszczególnych technik do wyznaczania podatności nitów. Udział poszczególnych rzędów nitów w przenoszeniu obciążenia określony został na drodze pomiarów tensometrycznych. Celem uwzględnia zjawiska wtórnego zginania tensometry oporowe mocowane były w rejonie zakładki parami tj. na wewnętrznej i zewnętrznej powierzchni jednej z łączonych blach. Stwierdzono nieco mniejszą podatność nitów w środkowym rzędzie połączenia w porównaniu z rzędami skrajnymi. Jakkolwiek w obu skrajnych rzędach podatności nitów były takie same, to transfer obciążenia przez każdy z nich był inny. Wyniki wykonanych wcześniej badań wskazują, że ten brak symetrii w transferze obciążenia może mieć związek ze znacznie większą ekspansją otworu nitowego w blasze po stronie zakuwki niż po stronie głowy fabrycznej. Wynika stąd, że zwykle stosowane procedury obliczeniowe uzależniające transfer obciążenia od samej tylko podatności nitów, prowadzić mogą do zafałszowanych wyników.